

## Multiphoton detachment of H<sup>-</sup>

Cecil Laughlin

*Department of Mathematics, Nottingham University, Nottingham NG7 2RD, England*

Shih-I Chu

*Department of Chemistry, University of Kansas, Lawrence, Kansas 66045*

(Received 25 June 1993)

Multiphoton detachment of H<sup>-</sup> is considered. An accurate one-electron model, which reproduces precisely the known H<sup>-</sup> detachment energy and the low-energy e-H(1s) elastic-scattering phase shifts, is developed. Generalized cross sections, based on lowest-nonvanishing-order perturbation theory, are evaluated by an accurate and efficient numerical algorithm for the solution of the associated set of inhomogeneous differential equations. Two- to eight-photon detachment cross sections are determined and compared with a recent one-electron model and two-electron *ab initio* calculations. It appears that the present study provides consistent results with an accuracy for higher-order ( $n > 3$ ) photon-detachment cross sections comparable to that of lower orders ( $n = 2, 3$ ). Average detachment rates for linearly polarized light are calculated and compared with recent experimental measurements. It is found that, for higher-order photon detachment, the rates for circular polarization are small in comparison with the rates for linear polarization.

PACS number(s): 32.80.Rm, 32.80.Fb

### I. INTRODUCTION

Experimental and theoretical investigations of the photodetachment of H<sup>-</sup> have a long history. However, recent experimental observations of multiphoton detachment of this fundamental negative ion [1–3] have given a renewed impetus to theoreticians to calculate H<sup>-</sup> multiphoton generalized cross sections and detachment rates [4]. As has been pointed out several times, wide discrepancies exist between many of the predictions, especially for two- and three-photon absorption processes which have occupied most of the theoretical interest so far.

There are several purposes to the present paper. The first is to introduce an accurate one-electron model of H<sup>-</sup> which is suitable for efficient multiphoton detachment calculations. Another is to develop stable and efficient numerical schemes capable of providing generalized cross sections, not only for two- and three-photon detachment, where there is now beginning to be a measure of agreement between different theoretical predictions, but also for four- to eight-photon detachment where the data, if they exist at all, are very sparse. This detailed and consistent calculation of high-order multiphoton cross sections for H<sup>-</sup> ( $n > 3$ ) which accurately takes into account the phase shifts of the detached electron. Finally, we use our results to calculate multiphoton detachment rates for comparison with the latest experimental measurements and we discuss the implications of the differences which this comparison shows for the future development of work in this area.

We begin in Sec. II with a brief review of the expressions for  $n$ -photon detachment generalized cross sections derived from perturbation theory and how they may be evaluated in terms of solutions of inhomogeneous

differential equations. In Sec. III we introduce our one-electron model of H<sup>-</sup> and verify its accuracy by comparing the predicted photodetachment cross section with that obtained in an accurate correlated two-electron study. Our model reproduces precisely the known H<sup>-</sup> detachment energy, recently shown to be very important for obtaining accurate generalized cross sections, and also the known *s*-, *p*-, *d*-, and *f*-wave low-energy e-H(1s) elastic-scattering phase shifts for the detached electron. We present in Sec. IV our numerical procedures for solving the set of inhomogeneous differential equations which replace the perturbation-theory summations and we show, by introducing a “perturbation” into the inhomogeneous terms, that they do not appear to suffer from any numerical instabilities. Section V contains our results for  $n$ -photon detachment of H<sup>-</sup> for  $n = 2–8$  and gives comparisons with other work, while Sec. VI contains our conclusions concerning the implications of the work on the future development of research in H<sup>-</sup> multiphoton detachment.

### II. PERTURBATION THEORY FOR MULTIPHOTON DETACHMENT OF NEGATIVE IONS

We consider  $n$ -photon detachment of an atomic negative ion, assuming that the light intensity is such that the ion-photon interaction may be treated as a perturbation and that the laser is monochromatic with frequency  $\omega$ . Then, to lowest order in perturbation theory, the probability per unit time that the system, initially in a bound state  $|b\rangle$ , will absorb  $n$  photons and make a transition to a final continuum state  $|f\rangle$ , ejecting a photoelectron in the solid angle  $d\Omega_k$  with momentum  $\mathbf{k}_f$  and is given by

$$dW_{fb}^{(n)} = (2\pi)^{n-2} \alpha^n \omega^n k_f |T_{fb}^{(n)}|^2 F^n d\Omega_k , \quad (1)$$

where  $F$  is the incident photon flux and  $T_{fb}^{(n)}$  is the transition-matrix element. (Unless otherwise stated, atomic units are used throughout this paper.) If the free ion has (discrete and continuous) states  $\phi_i$  with energies  $E_i$ , where

$$T_{fb}^{(n)} = \sum_{i_1, i_2, \dots, i_{n-1}} \frac{\langle \phi_f | \hat{\mathbf{e}} \cdot \mathbf{D} | \phi_{i_{n-1}} \rangle \langle \phi_{i_{n-1}} | \hat{\mathbf{e}} \cdot \mathbf{D} | \phi_{i_{n-2}} \rangle \cdots \langle \phi_{i_2} | \hat{\mathbf{e}} \cdot \mathbf{D} | \phi_{i_1} \rangle \langle \phi_{i_1} | \hat{\mathbf{e}} \cdot \mathbf{D} | \phi_b \rangle}{[E_{i_{n-1}} - E_b - (n-1)\omega][E_{i_{n-2}} - E_b - (n-2)\omega] \cdots (E_{i_2} - E_b - 2\omega)(E_{i_1} - E_b - \omega)}, \quad (3)$$

where  $\mathbf{D}$  is the electric dipole operator and the summations include integrations over continuous intermediate states  $\phi_{i_1}, \phi_{i_2}, \dots, \phi_{i_{n-1}}$ . In the case of H<sup>-</sup>, for which the ground state is the only true singlet bound state, all intermediate states are in the continuum. For  $n > 3$  it is not a practical procedure to evaluate the right-hand side of (3) by direct computation of the matrix elements [4]. Instead, we extend a method introduced by Dalgarno and Lewis [7] and discussed in the present context by, for example, Grontier and Trahin [8] and Gao and Starace [9]. A similar procedure has also been previously applied by us to multiphoton dissociation of H<sub>2</sub><sup>+</sup> and HD<sup>+</sup> from vibrationally excited states [10]. One of the goals of this work is to extend the Dalgarno-Lewis procedure [7] to high-order multiphoton processes in a numerically stable and efficient manner. The approach is to replace the intermediate-state summations and integrations in  $T_{fb}^{(n)}$  by a set of coupled inhomogeneous differential equations and one final integration. This is achieved by defining the functions

$$\chi_1 = \sum_{i_1} \frac{\langle \phi_{i_1} | \hat{\mathbf{e}} \cdot \mathbf{D} | \phi_b \rangle}{(E_{i_1} - E_b - \omega)} \phi_{i_1}, \quad (4a)$$

$$\chi_2 = \sum_{i_2} \frac{\langle \phi_{i_2} | \hat{\mathbf{e}} \cdot \mathbf{D} | \chi_1 \rangle}{(E_{i_2} - E_b - 2\omega)} \phi_{i_2}, \quad (4b)$$

:

$$\chi_{n-1} = \sum_{i_{n-1}} \frac{\langle \phi_{i_{n-1}} | \hat{\mathbf{e}} \cdot \mathbf{D} | \chi_{n-2} \rangle}{[E_{i_{n-1}} - E_b - (n-1)\omega]} \phi_{i_{n-1}} \quad (4c)$$

and noting that, by virtue of Eq. (2), they satisfy, respectively, the inhomogeneous differential equations

$$(\hat{H} - E_b - \omega)\chi_1 = \hat{\mathbf{e}} \cdot \mathbf{D}\phi_b, \quad (5a)$$

$$(\hat{H} - E_b - 2\omega)\chi_2 = \hat{\mathbf{e}} \cdot \mathbf{D}\chi_1, \quad (5b)$$

:

$$[\hat{H} - E_b - (n-1)\omega]\chi_{n-1} = \hat{\mathbf{e}} \cdot \mathbf{D}\chi_{n-2}. \quad (5c)$$

Having computed successively  $\chi_1, \chi_2, \dots, \chi_{n-1}$ , it is evident that

$$T_{fb}^{(n)} = \langle \phi_f | \hat{\mathbf{e}} \cdot \mathbf{D} | \chi_{n-1} \rangle. \quad (6)$$

The total transition probability  $W_{fb}$  is defined by integrating over all angles of the ejected electron and summing over all accessible final states,

$$\hat{H}\phi_i = E_i\phi_i, \quad (2)$$

and the photons have polarization specified by the unit vector  $\hat{\mathbf{e}}$ , then [5,6]

$$W_{fb}^{(n)} = (2\pi)^{n-2} \alpha^n \omega^n k_f F^n \sum_{l_f, m_f} \int |T_{fb}^{(n)}|^2 d\Omega_k, \quad (7)$$

where we have assumed that the initial bound state has an angular momentum  $l_b = 0$ , and  $l_f$  and  $m_f$  are final-state angular momentum quantum numbers. The quantity

$$\sigma^{(n)}(\omega) = W_{fb}^{(n)} / F^n \quad (8)$$

is the generalized  $n$ -photon detachment cross section, and we now turn our attention to its evaluation.

### III. MODEL POTENTIALS FOR H<sup>-</sup>

In order to simplify the solution of Eqs. (5) we introduce an angular-momentum-dependent model potential  $v_l(r)$  to describe the photoelectron, that is, we treat H<sup>-</sup> as an effective one-electron system in which the detached electron moves in the field of a perturbed hydrogen atom. The effective interaction between the detached electron and the bound electron is chosen to reproduce the binding energy of H<sup>-</sup> [11] and, also, the low-energy  $e$ -H(1s) singlet elastic-scattering phase shifts [12–15]. We note that since we are here describing the multiphoton detachment process using nonvanishing lowest-order perturbation theory, and since the binding energy of H<sup>-</sup> is relatively small (0.754 eV), it is adequate to have accurate representations of the *low-energy* phase shifts. Thus, we choose the following form for the model potential:

$$v_l(r) = - \left[ 1 + \frac{1}{r} \right] e^{-2r} - \frac{\alpha_d}{2r^4} W_6 \left[ \frac{r}{r_c} \right] + u_l(r), \quad (9)$$

where  $\alpha_d = \frac{9}{2}$  is the static polarizability of the hydrogen atom in its ground state,

$$W_j(x) = 1 - \exp(-x^j) \quad (10)$$

is a cutoff function, and  $r_c$  is an effective hydrogen-atom radius. The last term  $u_l(r)$  in (9) is an angular-momentum-dependent short-range correction of the form

$$u_l(r) = (c_0 + c_1 r + c_2 r^2) e^{-\beta r}, \quad (11)$$

where the coefficients  $c_0, c_1, c_2$ , and  $\beta$  are chosen to approximate as accurately as possible the binding energy [11] and low-energy singlet phase shifts [12–15] of H<sup>-</sup>. The values of the parameters thus determined are listed in Table I. We find it is sufficient to use 2 different functions  $u_l(r)$ : one,  $u_0(r)$ , for states with angular momentum  $l = 0$ , and another,  $u_1(r)$ , for states with  $l \geq 1$ . It is

TABLE I. Model-potential parameters [see Eqs. (9)–(11)].

$l$	$\alpha_d$	$r_c$	$c_0$	$c_1$	$c_2$	$\beta$
0	4.5	4.0	5.332 1766	-5.254 3795	0.420 0806	1.4
$\geq 1$	4.5	4.0	-2.302 0310	2.227 6939	-0.277 6654	1.4

also necessary to use two different functions because, for example,  $s$ - and  $p$ -wave phase shifts cannot be fitted with a common potentials  $v(r)$ . We also note that we have not included phase shifts  $\delta_l$  for  $l \geq 4$  in the fitting procedure to determine the parameters in  $u_1(r)$ . However,  $v_1(r)$  does reproduce values in agreement with the effective range formula [16]

$$\tan\delta_l = \frac{\pi\alpha_d k_f^2}{(2l-1)(2l+1)(2l+3)} \quad (12)$$

which is accurate at low energies for  $l \geq 4$ . The importance of employing the correct  $H^-$  binding energy has recently been emphasized by Liu, Gao, and Starace [17] and both of our potentials  $v_0(r)$  and  $v_1(r)$  reproduce the precise experimental value of Lykke, Murray, and Lineberger [11].

In calculations on the photodetachment of  $H^-$  in an electric field, Du and Delos [18] employed the initial-state wave function

$$\psi_b = B \exp(-\eta_b r)/r \quad (13)$$

where  $\eta_b$  is given in terms of the ground-state energy  $E_b$  of  $H^-$  (relative to the ground-state energy of hydrogen) by  $E_b = -\frac{1}{2}\eta_b^2$  and, following the prescription of Bethe and Longmire [19], the constant  $B$  is determined from the effective range of the potential energy [20]. This form of initial-state wave function has also been used by Adelman [21] to determine two-photon detachment rates for  $H^-$ . The value  $B = 0.315 52$  thus derived gives the normalization  $\langle \psi_b | \psi_b \rangle = 2.655$ . The asymptotic behavior of the model-potential ground-state wave function  $\phi_b$  [calculated with  $v_0(r)$ ] is described by Eq. (13) but, unlike  $\psi_b$ , it is normalized to unity. The lowest ( $l=0$ ) eigenvalue of  $v_1(r)$  also reproduces the binding energy of  $H^-$  exactly, but the corresponding wave function does not behave asymptotically like  $\phi_b$ ; instead it behaves as the normalized function

$$\theta_b = N \exp(-\eta_b r)/r, \text{ where } N = \left[ \frac{\eta_b}{2\pi} \right]^{1/2}, \quad (14)$$

for large  $r$ . The numerical value of  $N$  is 0.1936 and we note that  $B^2 = 2.655N^2$ .

Table II presents a comparison of our model-potential phase shifts with other accurate data. Agreement is satisfactory in all cases. Further validation of our model is provided by the good agreement shown in Table III between our predicted  $H^-$  photodetachment cross section and the cross section of Stewart [13], obtained from an accurate perturbation-variation method, and Wishart [22], who used a close-coupling pseudostate expansion with the addition of Hylleraas-type correlation terms. Our results favor those of Wishart [22].

We finally note in this section that consistent application of the model-potential theory implies the use of a dipole operator  $\mathbf{D}$  which includes the contribution from the dipole moment induced on the hydrogen-atom “core” by the “valence” electron [23,24]

$$\mathbf{D} = \left[ 1 - \frac{\alpha_d}{r^3} W_3 \left[ \frac{r}{r_c} \right] \right] \mathbf{r}. \quad (15)$$

Because our wave functions are correct asymptotically, the “length” form of the dipole operator, given in Eq. (15), is appropriate.

#### IV. CALCULATIONS

We now solve sequentially the set of inhomogeneous differential equations (5) for  $\chi_1, \chi_2, \dots, \chi_{n-1}$ , where the Hamiltonian  $\hat{H}$  is given by

$$\hat{H} = \frac{1}{2}\nabla^2 + v_l(r), \quad (16)$$

with the model potentials  $v_l(r)$  specified by Eqs. (9)–(11). This allows computation of the generalized cross sections  $\sigma^{(n)}(\omega)$  defined in (8), via Eqs. (6) and (7). We also repeat, and extend to  $n=8$ , calculations with a zero-range potential model introduced by Geltman [25].

#### A. Solution of inhomogeneous differential equations

If the eigenfunctions  $\phi_{l_\mu}$  in the definition of  $\chi_\mu$  ( $\mu = 1, 2, \dots, n-1$ ), Eqs. (4), have angular-momentum quantum numbers  $l = l_\mu$  and  $m = m_\mu$ , then the substitution  $\chi_\mu = r^{-1} P_\mu(r) Y_{l_\mu m_\mu}(\hat{\mathbf{r}})$  reduces the equation for  $\chi_\mu$  to the second-order ordinary differential equation

TABLE II.  $e$ - $H$ (1s) singlet elastic-scattering phase shifts as a function of electron energy (in a.u.).

Angular momentum	Energy	Model potential	Accurate calculation <sup>a</sup>
$l=0$	0.005	2.5532	2.5530
	0.020	2.0666	2.0673
	0.045	1.6971	1.6964
$l=1$	0.005	0.0065	0.0058
	0.010	0.0108	0.0100
	0.020	0.0155	0.0146
	0.040	0.0161	0.0164
$l=2$	0.005	0.0013	0.0012
	0.020	0.0051	0.0052
	0.045	0.0101	0.0108
	0.045	0.0040	0.0038
$l=3$	0.080	0.0069	0.0066

<sup>a</sup>See Refs. [12–15].

TABLE III. H<sup>-</sup> photodetachment cross sections (in units of  $10^{-17}$  cm<sup>2</sup>) as a function of electron energy (in a.u.).

Energy	Model potential	Cross section Stewart <sup>a</sup>	Wishart <sup>b</sup>
0.005	1.57	1.54	1.55
0.010	2.86	2.82	2.85
0.015	3.58	3.52	
0.020	3.91	3.85	3.90
0.025	4.01	3.94	
0.030	3.98	3.90	3.97
0.035	3.87	3.78	
0.040	3.72	3.62	3.71
0.050	3.37	3.27	3.37

<sup>a</sup>Reference [13].

<sup>b</sup>Reference [22].

$$\left[ \frac{d^2}{dr^2} - \frac{l_\mu(l_\mu+1)}{r^2} - 2v_{l_\mu}(r) + 2(E_b + \mu\omega) \right] P_\mu = -2\alpha_q DP_{\mu-1}, \quad (17)$$

where  $\hat{\mathbf{e}} \cdot \mathbf{D} = DC_{1q}(\hat{\mathbf{r}})$  and

$$\alpha_q = \langle Y_{l_\mu m_\mu}(\hat{\mathbf{r}}) | C_{1q}(\hat{\mathbf{r}}) | Y_{l_{\mu-1} m_{\mu-1}}(\hat{\mathbf{r}}) \rangle. \quad (18)$$

For convenience, we define  $\chi_0 = \phi_b$ . Equation (17) may be integrated numerically by use of the Numerov method [26]. The matrix formulation described by Froese Fischer [27] was employed in the present work. The boundary conditions are  $P_\mu(0)=0$  and  $P_\mu(r) \rightarrow 0$  as  $r \rightarrow \infty$ . In practice, the equation was integrated in the interval  $0 \leq r \leq R$ , where  $R$  is sufficiently large that  $|P_\mu(r)| < \epsilon$  for  $r > R$  and  $\epsilon$  is a suitably chosen (small) parameter.

In our model, the ground state of H<sup>-</sup> has an angular momentum  $l=0$ . When the laser has circular polarization it follows that  $l_\mu$  in Eq. (17) must have the value  $l_\mu = \mu$  and that the angular momentum of the ejected photoelectron is  $l_f = n$ , the number of photons absorbed. However, for linear polarization several values of  $l_\mu$  are, in general, possible and thus there are several functions  $P_\mu$  to be found. For example, the four-photon detachment with a linearly polarized laser the following angular-momentum paths are possible:

$$0 \rightarrow 1 \rightarrow 2 \rightarrow 3 \rightarrow 4, \quad (19a)$$

$$0 \rightarrow 1 \rightarrow 2 \rightarrow 3 \rightarrow 2, \quad (19b)$$

$$0 \rightarrow 1 \rightarrow 2 \rightarrow 1 \rightarrow 2, \quad (19c)$$

$$0 \rightarrow 1 \rightarrow 2 \rightarrow 1 \rightarrow 0, \quad (19d)$$

$$0 \rightarrow 1 \rightarrow 0 \rightarrow 1 \rightarrow 2, \quad (19e)$$

$$0 \rightarrow 1 \rightarrow 0 \rightarrow 1 \rightarrow 0. \quad (19f)$$

It is clear that if the number  $n$  of photons is even then the final continuum states have angular momenta  $l_f$  which are also even, and *vice versa* if  $n$  is odd. It is also clear that there is only one function  $P_1$  (with  $l_1=1$ ), but that there are two functions  $P_2$ , namely  $P_2$  ( $l_2=2$ ) and  $P_2$

( $l_2=0$ ), and three functions  $P_3$ , one of which has  $l_3=3$  and two of which have  $l_3=1$ . The number of angular-momentum paths is given by the binomial coefficient  $\binom{n}{h}$ , where  $h = [n/2]$  is the integer part of  $n/2$ . The calculations are obviously most efficiently executed by first determining  $P_1$ , then the two functions  $P_2$  (both of which depend on  $P_1$ ), then the three functions  $P_3$ , etc. For eight-photon detachment, where there are 70 angular-momentum paths and, in total,  $1+2+3+6+10+20+35=77$  inhomogeneous differential equations to solve, the time required to calculate  $\sigma^{(8)}$  on a VAX-6410 computer was approximately 12 seconds per laser frequency. Thus, the procedure developed in this work is highly efficient and can be extended to multiphoton processes of even higher order.

## B. Multiphoton detachment cross sections

Generalized cross sections  $\sigma^{(n)}$  for  $n$ -photon detachment of H<sup>-</sup> were calculated as described above for photon energies in the range  $-E_b/n < \omega < -E_b/(n-1)$  for each  $n=2, \dots, 8$ . Results for linear laser polarization are presented in Figs. 1–7. We also performed calculations in which the model potentials  $v_l(r)$  were set equal to zero, so that the initial bound-state wave function is the normalized function  $\theta_b$  of Eqs. (14) and the final states are plane waves, and these results are also displayed in Figs. 1–7. This approximation, the *zero-range plane-wave* (ZRPW) model, has been employed by Geltman [25] to obtain generalized cross sections for two- to seven-photon detachment of H<sup>-</sup>. Geltman used a completely different calculational method and the agreement of our ZRPW results with his provides validation for our numerical procedures. Following the prescription of Geltman [4] we have multiplied our ZRPW cross sections by a factor of 2 to account for both equivalent electrons in H<sup>-</sup>.

It has been suggested that the sequence of coupled differential equations, (5a)–(5c), may eventually become numerically unstable as the order of the photon process  $n$

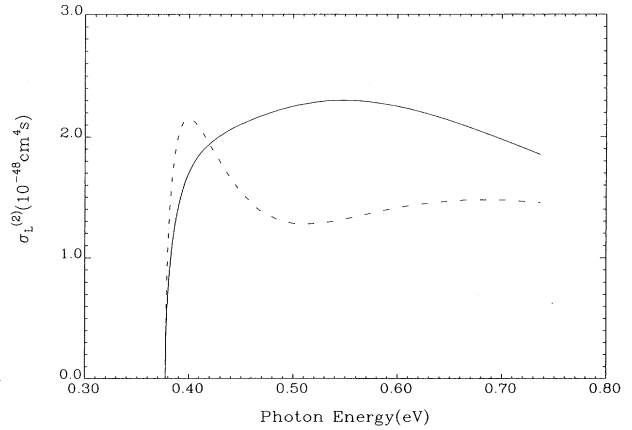


FIG. 1. Generalized cross sections  $\sigma_L^{(2)}$  for two-photon detachment of H<sup>-</sup> using linearly polarized light plotted vs photon energy. Solid curve: present model-potential calculation. Dashed-dotted curve: ZRPW results.

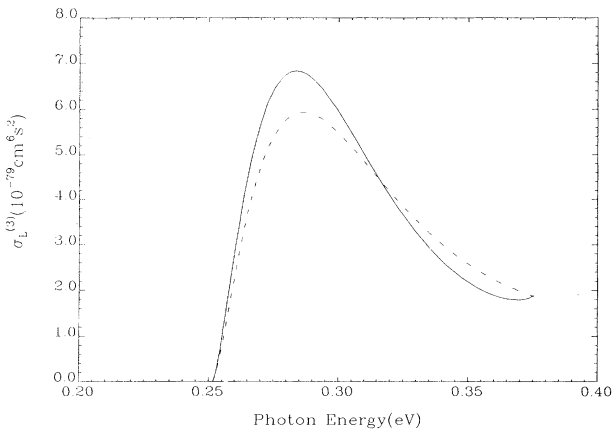


FIG. 2. Generalized three-photon detachment cross sections  $\sigma_L^{(3)}$ . Solid curve: present model-potential calculation. Dashed-dotted curve: ZRPW results.

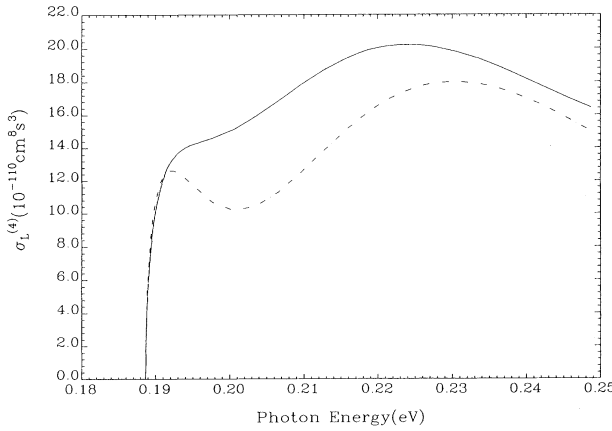


FIG. 3. Generalized four-photon detachment cross sections  $\sigma_L^{(4)}$ . Solid curve: present model-potential calculation. Dashed-dotted curve: ZRPW results.

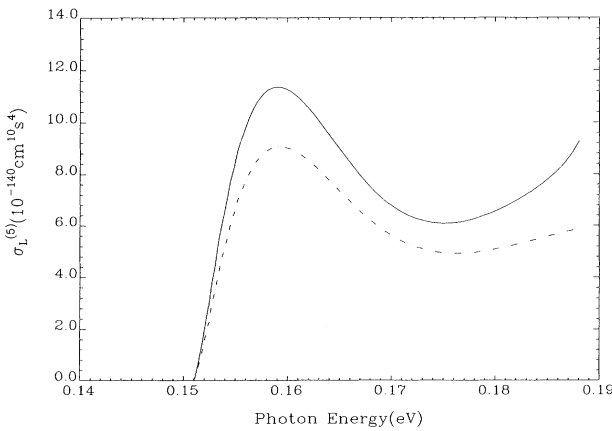


FIG. 4. Generalized five-photon detachment cross sections  $\sigma_L^{(5)}$ . Solid curve: present model-potential calculation. Dashed-dotted curve: ZRPW results.

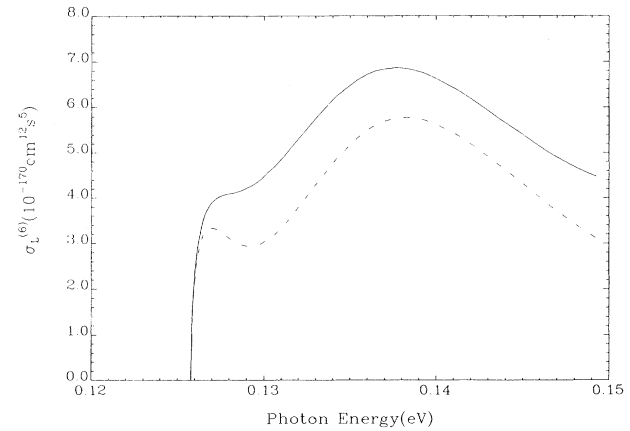


FIG. 5. Generalized six-photon detachment cross sections  $\sigma_L^{(6)}$ . Solid curve: present model-potential calculation. Dashed-dotted curve: ZRPW results.

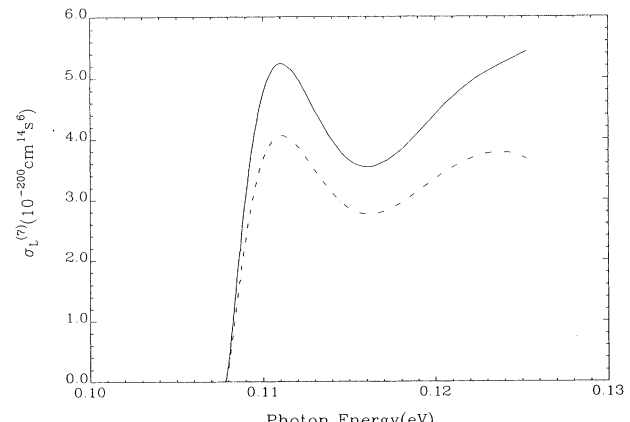


FIG. 6. Generalized seven-photon detachment cross sections  $\sigma_L^{(7)}$ . Solid curve: present model-potential calculation. Dashed-dotted curve: ZRPW results.

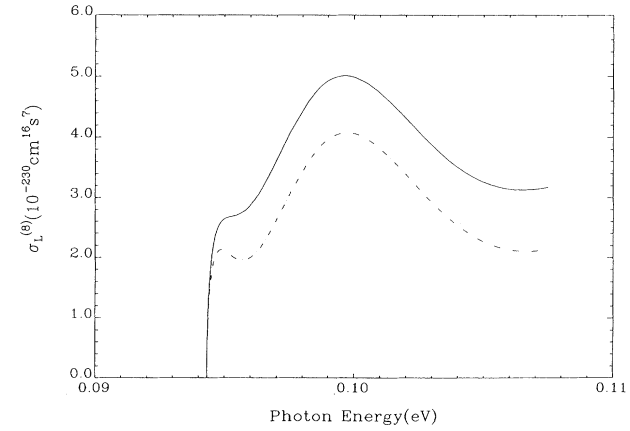


FIG. 7. Generalized eight-photon detachment cross sections  $\sigma_L^{(8)}$ . Solid curve: present model-potential calculation. Dashed-dotted curve: ZRPW results.

is increased [28]. This is because an error in  $\chi_\mu$ , for example, is fed into the right-hand side of the equation for  $\chi_{\mu+1}$  and errors are thus propagated to the higher equations. Gao and Starace [28] have proposed a variationally stable procedure to overcome any such unstable behavior in the solution of equations (5) and applications of their procedure to multiphoton processes have been made [9,29]. However, we have not found any evidence of instability in Eqs. (5) in our calculations on H<sup>-</sup>. As well as the dipole operator  $\mathbf{D}$  given by Eq. (15), modified to include polarization effects, we have also used the unmodified dipole operator  $\mathbf{D}_0 = \mathbf{r}$ . If the inhomogeneous differential equations were sensitive to errors in the right-hand-side terms, then it would be expected that the perturbations introduced by the polarization term

$$\mathbf{D}_1 = -\frac{\alpha_d}{r^3} W_3 \left[ \frac{r}{r_c} \right] \mathbf{r} \quad (20)$$

in  $\mathbf{D}$  would result in progressively larger differences between the two sets of generalized cross sections (calculated with  $\mathbf{D}_0$  and  $\mathbf{D}$ , respectively) as the photon number  $n$  increased. Large differences were not found. Generalized cross sections for three- and eight-photon detachment are presented in Tables IV and V, where it will be observed that the relative changes on replacing the dipole operator  $\mathbf{D}_0$  by  $\mathbf{D} = \mathbf{D}_0 + \mathbf{D}_1$  are small and are approximately the same in both cases.

## V. RESULTS AND DISCUSSIONS

Several authors have calculated the generalized cross sections  $\sigma_L^{(2)}(\omega)$  and  $\sigma_L^{(3)}(\omega)$  for H<sup>-</sup>; work on  $\sigma_L^{(n)}(\omega)$  for  $n > 3$  is much more limited. We do not discuss all the available calculations but limit ourselves in the main to the more recent results. Also, we concentrate on cross sections  $\sigma_L^{(n)}(\omega)$  for multiphoton detachment by linearly polarized light since circular-polarization cross sections  $\sigma_C^{(n)}(\omega)$  diminish rapidly relative to  $\sigma_L^{(n)}(\omega)$  as  $n$  increases.

### A. Generalized cross sections

Figures 1–7 show that the discrepancies between model-potential and ZRPW generalized multiphoton detachment cross sections  $\sigma_L^{(n)}$  are greatest for even values of  $n$ , where interference effects in the ZRPW cross sections are clearly evident. This is due to the fact that the phase shifts are largest for  $l=0$ , but are taken to the zero in the ZRPW model, and final continuum states with  $l_f=0$  are accessible only when  $n$  is even. When the correct *s*-wave phase shifts are incorporated into the model then the accuracy of the cross sections improves dramatically [4].

It may also be noted that, for  $n$  odd, ZRPW and model-potential  $\sigma_L^{(n)}$ 's would generally be in better agreement if the initial-state wave function  $\psi_b$  given by Eq. (13) was used in the ZRPW calculations, rather than the wave function  $\theta_b$  of (14) together with the factor of 2 (to account for the two equivalent electrons) mentioned above. Since the normalization of (13) is  $\langle \psi_b | \psi_b \rangle = 2.655$ , this prescription would increase the ZRPW generalized cross sections by approximately 30% and bring them closer to the model-potential  $\sigma_L^{(n)}$ 's, in agreement with the observations of Geltman [4] and Liu, Gao, and Starace [17] for  $n=2$  and 3.

We compare our generalized cross sections for two- and three-photon detachment of H<sup>-</sup> by linearly polarized light with Geltman's "model" and "best-phase" results [4] and with the semi-empirical adiabatic hyperspherical results of Liu, Gao, and Starace [17] in Figs. 8 and 9. It is evident that our model-potential results are in closer accord with Geltman's best phase than with his model results; the former results of Geltman are expected to be more accurate [4]. We note a slight difference in behavior at the top end of the photon-energy range. As the laser-photon energy is increased, the final function  $\chi_{n-1}$ , Eq. (5c), becomes more diffuse and the upper limit  $R$  of the integration range needs to become quite large in order to meet the condition  $|P_\mu(r)| < \epsilon$  for  $r > R$  introduced earlier. Thus, the region close to the ( $n-1$ )-photon threshold is the most difficult to deal with numer-

TABLE IV. Generalized cross sections  $\sigma_L^{(3)}$  (in units of  $10^{-79} \text{ cm}^6 \text{ sec}^2$ ) for three-photon detachment of H<sup>-</sup> by linearly polarized light.  $\sigma_L^{(3)}(0)$  is calculated with the dipole operator  $\mathbf{D}_0 = \mathbf{r}$  and  $\sigma_L^{(3)}(3)$  with the dipole operator  $\mathbf{D}$  corrected for polarization effects [Eq. (15)].  $\rho = \sigma_c^{(3)}/\sigma_L^{(3)}$  is the ratio of detachment rates for circularly and linearly polarized light. The number in brackets indicates the power of 10 by which the entry is to be multiplied.

Photon energy (cm <sup>-1</sup> )	$\sigma_L^{(3)}(0)$	$\sigma_L^{(3)}(3)$	$\rho(0)$	$\rho(3)$
2076	1.908	1.896	1.79[-3]	1.80[-3]
2173	5.604	5.565	1.90[-2]	1.90[-2]
2269	6.867	6.813	6.26[-2]	6.28[-2]
2366	6.525	6.467	1.47[-1]	1.48[-1]
2462	5.505	5.450	2.93[-1]	2.94[-1]
2559	4.360	4.312	5.28[-1]	5.31[-1]
2655	3.358	3.317	8.82[-1]	8.86[-1]
2752	2.595	2.563	1.37	1.37
2848	2.089	2.063	1.93	1.93
2945	1.835	1.815	2.40	2.40

TABLE V. As Table IV, but for  $\sigma_L^{(8)}$  (in units of  $10^{-230} \text{ cm}^{16} \text{ sec}^7$ ). The number in brackets indicates the power of 10 by which the entry is to be multiplied.

Photon energy (cm <sup>-1</sup> )	$\sigma_L^{(8)}(0)$	$\sigma_L^{(8)}(3)$	$\rho(0)$	$\rho(3)$
765.5	2.643	2.634	8.96[-13]	8.98[-13]
775.9	3.032	3.021	6.45[-9]	6.46[-9]
786.2	4.100	4.086	2.68[-7]	2.68[-7]
796.6	4.890	4.873	2.88[-6]	2.88[-6]
806.9	4.992	4.975	1.76[-5]	1.76[-5]
817.3	4.593	4.577	7.75[-5]	7.77[-5]
827.6	4.023	4.008	2.72[-4]	2.72[-4]
838.0	3.531	3.516	7.77[-4]	7.78[-4]
848.3	3.233	3.218	1.84[-3]	1.84[-3]
858.7	3.140	3.126	3.64[-3]	3.65[-3]

ically. To ensure that we obtained numerical convergence in our calculations we varied both  $\epsilon$  and the step length in the numerical integration routine.

There is quite reasonable agreement between our model-potential generalized multiphoton detachment cross sections and the semiempirical adiabatic hyperspherical predictions of Liu, Gao, and Starace [17]. These authors introduced a semiempirical adjustment to bring their predicted attachment energy of H<sup>-</sup> into exact agreement with the accurate nonrelativistic value of Pekeris [30], and they discovered that this adjustment substantially reduced (by up to 40%) the two- and three-photon detachment cross sections. Nevertheless, their final cross sections are still 10–15 % larger than ours.

Our two-photon cross sections are in close agreement with those obtained by Adelman [21] (corrected, as pointed out by Geltman [4], by a factor of 2) from an asymptotic model. When we compare with *ab initio* two-electron calculations some significant discrepancies appear. Thus, agreement of our multiphoton detachment

cross sections  $\sigma_L^{(n)}$  with those obtained very recently by Proulx and Shakeshaft [31] is reasonable ( $n=2, 3$ ), but it is not so good, especially near threshold, when we compare with the results of Mercouris and Nicolaides [32] ( $n=2, 3, 4$ ), and the generalized cross sections calculated by Crance [33] are factors of up to 2 to 3 smaller than ours for  $n=2$  and 3, with even larger discrepancies for  $n=4$  and 5. For the sake of clarity we do not display all these results in Figs. 8 and 9 (see Ref. [17] for additional comparisons). An explicit two-electron treatment of multiphoton detachment of H<sup>-</sup> presents formidable difficulties, especially for processes involving absorption of more than two or three photons, and the results of the calculations mentioned above are in substantial disagreement. On the other hand, there is now reasonably good agreement between the results of recent model calculations for two- and three-photon detachment and, since our model potential accurately captures initial-, intermediate-, and final-state correlations, we feel that the resulting generalized multiphoton cross sections are currently the best available. We mention again the large discrepancy between the adiabatic hyperspherical and the semiempirical adiabatic hyperspherical results of Liu, Gao, and Starace [17] for  $\sigma_L^{(2)}$  and  $\sigma_L^{(3)}$  and note that

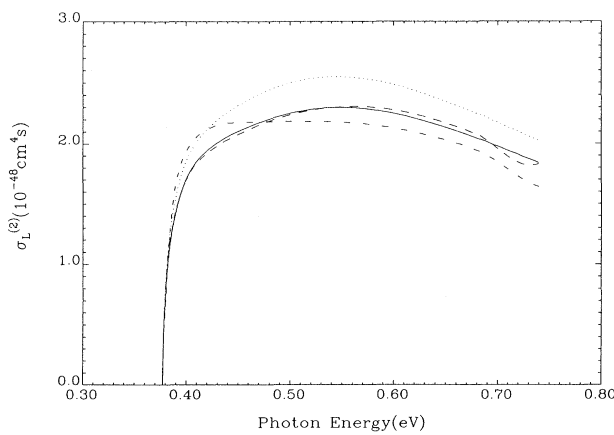


FIG. 8. Comparison of calculated  $\sigma_L^{(2)}$  for linear polarization. Solid curve: present model potential results. Dashed curve: Geltman's "best-phase" approximation results [4]. Dashed-dotted curve: Geltman's "model" approximation results [4]. Dotted curve: semiempirical adiabatic hyperspherical results [17].

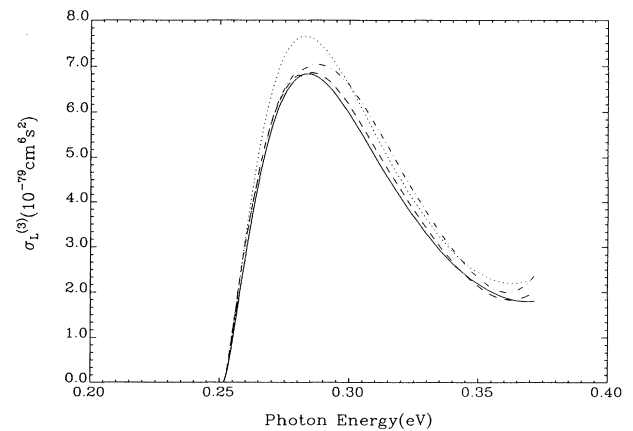


FIG. 9. Comparison of calculated  $\sigma_L^{(3)}$  for linear polarization. Curve notation same as Fig. 8.

these authors considered their latter calculations, with which we are in much better agreement, to be much more reliable.

We observed earlier that for linear polarization of the laser the angular momentum of the ejected photoelectron will be even or odd depending on whether the number of laser photons absorbed is, respectively, even or odd. It therefore follows from the Wigner threshold law [34]

$$\sigma_L^{(n)} \propto (E_b + n\omega)^{l_0+1/2}, \quad (21)$$

where  $l_0$  is the smallest of the final-state angular-momentum quantum numbers  $l_f$  (i.e., either 0 or 1), that the shape of cross sections at threshold will be qualitatively different for even- and odd-photon detachment [4]. Our calculations reveal that the cross sections near threshold are dominated by the lowest- $l$  partial waves and, hence, we should expect to observe obvious differences in cross-section behavior near threshold. That such differences are not immediately apparent from Figs. 1–7 is due to the fact that the Wigner law holds only very close to threshold. We illustrate the threshold behavior of the four- and five-photon cross sections in Figs. 10 and 11 in a much expanded (photon) energy range. In common with Geltman [4], we note that our threshold behavior is not quite in perfect accord with experiment [1,3]. This is partly due to the fact that the ac Stark shift of the ground state and the laser intensity-dependent effects are not included in these perturbative calculations.

We also note that because of the observed dominance of low- $l$  partial waves, cross sections for circular polarization become progressively smaller relative to linear-polarization cross sections as the number of photons required for detachment is increased, i.e., the ratio  $\rho = \sigma_C^{(n)} / \sigma_L^{(n)}$  of  $n$ -photon detachment rates for circularly and linearly polarized light decreases as  $n$  increases.

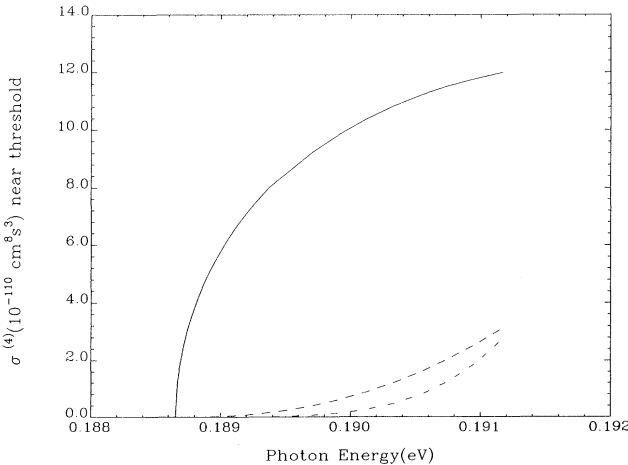


FIG. 10. Threshold behavior of four-photon detachment partial cross sections of H<sup>-</sup> by linearly polarized light. Solid curve:  $l=0$ . Dashed curve:  $l=2$ . Dashed-dotted curve  $l=4$ . The partial cross sections  $\sigma_L^{(4)}$  are multiplied by a factor of 10 for  $l=2$  and by  $10^5$  for  $l=4$ .

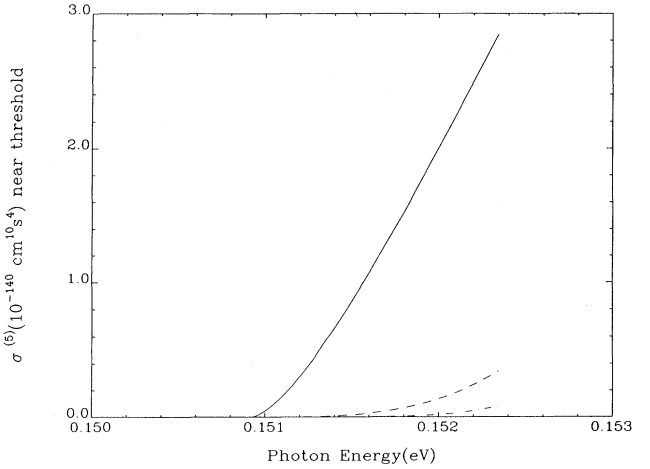


FIG. 11. Threshold behavior of five-photon detachment partial cross sections of H<sup>-</sup> by linearly polarized light. Solid curve:  $l=1$ . Dashed curve:  $l=3$ . Dashed-dotted curve:  $l=5$ . The partial cross sections  $\sigma_L^{(5)}$  are multiplied by a factor of  $10^2$  for  $l=3$  and by  $10^6$  for  $l=5$ .

However,  $\rho$  increases quite rapidly with photon energy  $\omega$  (see, for example, Tables IV and V).

### B. Multiphoton detachment rates

We now use our calculated generalized cross sections to obtain H<sup>-</sup> multiphoton detachment rates to compare with experimental measurements [3] which give averaged rates  $\bar{\Gamma}(\omega)$  versus photon energy  $\omega$  for various peak laser intensities  $I_p$ . Straightforward application of the formula

$$\bar{\Gamma}(\omega) = \sum_{n \geq n_p} \sigma^{(n)}(\omega) F^n, \quad (22)$$

where  $n_p$  is the minimum number of photons needed for detachment at (monochromatic) laser frequency  $\omega$  and the photon flux  $F = I_p / \omega$ , results in detachment rates substantially larger than those observed experimentally. It is therefore necessary to average our theoretical rates to bring them into quantitative agreement with measured rates. We achieve this by following the prescription of Geltman [4]: that is, we assume a Gaussian laser pulse whose intensity at distance  $R$  from the beam axis is given by

$$I(R) = I_p \exp \left[ - \left( \frac{R}{\gamma} \right)^2 \right] \quad (23)$$

and average over displacements  $R$  of H<sup>-</sup> ions from the beam axis from  $R=0$  to  $R=R_m$ . This results in

$$\begin{aligned} \bar{\Gamma}(\omega) &= \frac{\gamma^2}{R_m^2} \sum_{n \geq n_p} \sigma^{(n)}(\omega) \frac{I_p^n}{n \omega^n} \\ &\times \left\{ 1 - \exp \left[ -n \left( \frac{R_m}{\gamma} \right)^2 \right] \right\}. \end{aligned} \quad (24)$$

Note that the factor  $\{1 - \exp[-n(R_m/\gamma)^2]\}$  in the numerator of this equation would appear to be in the

denominator in Eq. (32) of Ref. [4]. The ratio  $\gamma/R_m$  is an effective scale factor and choosing its value to be 0.7 gives best agreement with observed rates.

Multiphoton detachment rates  $\bar{\Gamma}(\omega)$  have been measured by Tang *et al.* [3] for peak (laboratory) laser intensities of 4, 6, and 12 GW/cm<sup>2</sup>. Results derived from our model-potential multiphoton detachment cross sections for 4 GW/cm<sup>2</sup> are presented in Fig. 12 in comparison with the experimental data for photon energies in the range 0.18–0.39 eV. It is not clear for what range of intensities the perturbation theory is valid in the present application, so here we concentrate on the lowest intensity (i.e., 4 GW/cm<sup>2</sup>) for which experimental measurements are currently available. Our results for laser intensities of 6 and 12 GW/cm<sup>2</sup> do not differ appreciably from those presented by Geltman [4].

Figure 12 shows that while the theoretical results for the absolute rates  $\bar{\Gamma}$  agree with the measurement well within the estimated experimental uncertainty [3] of a factor of 5, there is one major discrepancy, namely, the experimental data do not show the sharpness of the onset of  $n$ -photon thresholds indicated in the theoretical curve. As also pointed out by Geltman [4], this could be an indication that nonperturbative treatments of this process are needed in this laser intensity region ( $I \geq 4$  GW/cm<sup>2</sup>). In our view, discrepancies between theoretical and current experimental data will not be removed by more refined (*ab initio*) calculations of generalized cross sections within a perturbation-theory regime; there is now sufficient agreement between various theoretical calculations to rule out this possibility.

## VI. CONCLUSION

In this paper, we have (i) constructed an accurate one-electron model potential for H<sup>-</sup>, taking into account accurately the binding energy and the low-energy  $e$ -H(1s) elastic-scattering phase shifts for the detached electron; (ii) developed efficient and stable numerical procedures for the accurate solution of the set of inhomogeneous differential equations; (iii) determined for the first time  $n$ -photon detachment cross sections of H<sup>-</sup> (for  $n = 2-8$ ) in

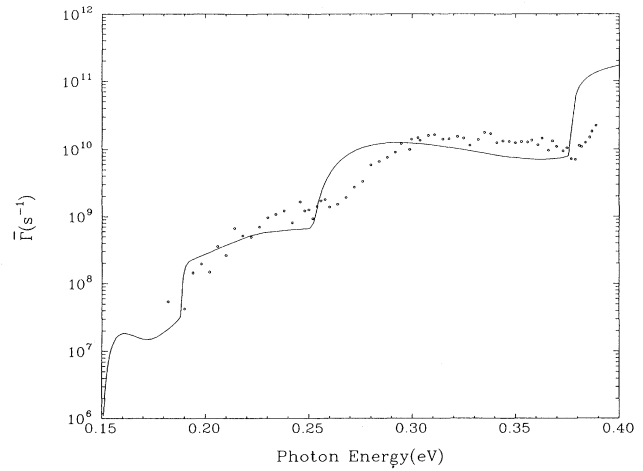


FIG. 12. Comparison of experimental [3] and presently calculated average multiphoton-detachment rates for linearly polarized Gaussian pulses with peak laboratory-frame intensity of 4 GW/cm<sup>2</sup>.

an accurate and consistent manner for all orders being considered; and (iv) made comparisons with available experimental and theoretical data.

We found that the nonperturbative treatment of multiphoton detachment of H<sup>-</sup> is likely to be important. Extension of the non-Hermitian Floquet formalism [35] for nonperturbative study is currently underway. Intensity-dependent generalized cross sections  $\sigma^{(n)}$  and intensity-dependent threshold behavior will be explored in detail.

## ACKNOWLEDGMENTS

This work was partially supported by the Division of Chemical Sciences, Office of Basic Energy Sciences of the U.S. Department of Energy. We are grateful to Dr. Geltman and Dr. Starace for providing their theoretical data and to Dr. Bryant for providing the experimental data for the comparison with the present work.

- 
- [1] C. Y. Tang, P. G. Harris, A. H. Mohagheghi, H. C. Bryant, C. R. Quick, J. B. Donahue, R. A. Reeder, S. Cohen, W. W. Smith, and J. E. Stewart, Phys. Rev. A **39**, 6068 (1989).
  - [2] W. W. Smith, C. Y. Tang, C. R. Quick, H. C. Bryant, P. G. Harris, A. H. Mohagheghi, J. B. Donahue, R. A. Reeder, H. Sharifian, J. E. Stewart, H. Toutounchi, S. Cohen, T. C. Altman, and D. C. Rislove, J. Opt. Soc. Am. B **8**, 17 (1991).
  - [3] C. Y. Tang, H. C. Bryant, P. G. Harris, A. H. Mohagheghi, R. A. Reeder, H. Sharifian, H. Tootoonchi, C. R. Quick, J. B. Donahue, S. Cohen, and W. W. Smith, Phys. Rev. Lett. **66**, 3124 (1991).
  - [4] For a summary of recent work and a more complete list of references in this direction, see S. Geltman, Phys. Rev. A **43**, 4930 (1991).
  - [5] H. B. Bebb and A. Gold, Phys. Rev. **143**, 1 (1966).
  - [6] P. Lambropoulos, Adv. At. Mol. Phys. **12**, 87 (1976).
  - [7] A. Dalgarno and J. T. Lewis, Proc. R. Soc. London Ser. A **233**, 70 (1955).
  - [8] Y. Gontier and M. Trahin, Phys. Rev. **172**, 83 (1968).
  - [9] B. Gao and A. F. Starace, Phys. Rev. A **39**, 4550 (1989).
  - [10] S. I. Chu, C. Laughlin, and K. K. Datta, Chem. Phys. Lett. **98**, 476 (1983); C. Laughlin, K. K. Datta, and S. I. Chu, J. Chem. Phys. **85**, 1403 (1986).
  - [11] K. R. Lykke, K. K. Murray and W. C. Lineberger, Phys. Rev. A **43**, 6104 (1991).
  - [12] C. Schwartz, Phys. Rev. **124**, 1468 (1961).
  - [13] A. L. Stewart, J. Phys. B **11**, 3851 (1978).
  - [14] M. R. H. Rudge, J. Phys. B **8**, 940 (1975).
  - [15] J. Callaway, Phys. Lett. **A65**, 199 (1978).
  - [16] T. F. O'Malley, L. Spruch, and L. Rosenberg, J. Math.

- Phys. **2**, 421 (1961).
- [17] C. R. Liu, B. Gao, and A. F. Starace, Phys. Rev. A **46**, 5985 (1992).
- [18] M. L. Du and J. B. Delos, Phys. Rev. A **38**, 5609 (1988).
- [19] H. A. Bethe and C. Longmire, Phys. Rev. **77**, 647 (1950).
- [20] T. Ohmura and H. Ohmura, Phys. Rev. **118**, 154 (1960).
- [21] S. A. Adelman, J. Phys. B **6**, 3851 (1973).
- [22] A. W. Wishart, J. Phys. B **12**, 3511 (1979).
- [23] I. B. Bersuker, Opt. Spectrosc. **3**, 97 (1957).
- [24] S. Hameed, A. Herzenberg, and M. G. James, J. Phys. B **1**, 822 (1988).
- [25] S. Geltman, Phys. Rev. A **42**, 6958 (1990).
- [26] C-E. Fröberg, *Introduction to Numerical Analysis* (Addison-Wesley, Reading, MA, 1965).
- [27] C. Froese Fischer, *The Hartree-Fock Method for Atoms: A Numerical Approach* (Wiley, New York, 1977).
- [28] B. Gao and A. F. Starace, Phys. Rev. Lett. **61**, 404 (1988).
- [29] B. Gao, Cheng Pan, Chih-Ray Liu, and A. F. Starace, J. Opt. Soc. Am. B **7**, 622 (1990).
- [30] C. L. Perkeris, Phys. Rev. **126**, 1470 (1962).
- [31] D. Proulx and R. Shakeshaft, Phys. Rev. A **46**, R2221 (1992).
- [32] (a) Th. Mercouris and C. A. Nicolaides, J. Phys. B **23**, 2037 (1990); (b) **24**, L165 (1991); (c) Phys. Rev. A **45**, 2116 (1992).
- [33] M. Crance, J. Phys. B **23**, L286 (1990); **24**, L169 (1991).
- [34] E. P. Wigner, Phys. Rev. **73**, 1002 (1948).
- [35] For a recent review on non-Hermitian Floquet methods, see, S. I. Chu, Adv. Chem. Phys. **73**, 739 (1989).